Supporting Information for

Modifications in Coordination Structure of $Mg[TFSA]_2$-Based Supporting Salts for High-Voltage Magnesium Rechargeable Batteries

Toshihiko Mandai,[1,2,§,] Kenji Tatesaka,[1] Kenya Soh,[3] Hyuma Masu,[4] Ashu Choudhary,[5] Yoshitaka Tateyama,[2,5] Ryuta Ise,[6] Hiroaki Imai,[6] Tatsuya Takeguchi,[1] and Kiyoshi Kanamura[3]*

[1]Department of Chemistry and Biological Sciences, Faculty of Science and Engineering, Iwate University, Ueda 4-3-5, Morioka 020-8551, Japan

[2]Global Research Center for Environment and Energy based on Nanomaterials Science (GREEN), National Institute for Materials Science (NIMS), 1-1 Namiki, Tsukuba, Ibaraki 305-0044, Japan

[3]Department of Applied Chemistry, Tokyo Metropolitan University, 1-1 Minami-Osawa, Hachioji, Tokyo 192-0397, Japan

[4]Center for Analytical Instrumentation, Chiba University, 1-33 Yayoi-cho, Inage-ku, Chiba 263-8522, Japan

[5]Center for Materials Research by Information Integration (CMI2), Research and Services Division of Materials Data and Integrated System (MaDIS), National Institute for Materials Science (NIMS), 1-2-1 Sengen, Tsukuba, Ibaraki, 305-0047, Japan

[6]Department of Applied Chemistry, Faculty of Science and Technology, Keio University, 3-14-1 Hiyoshi, Kohoku-ku, Yokohama 223-8522, Japan

[§]Present address: Research Center for Energy and Environmental Materials, National Institute for Materials Science (NIMS), 1-1 Namiki, Tsukuba, Ibaraki 305-0044, Japan

CORRESPONDING AUTHOR FOOTNOTES

Telephone: +81-29-860-4464, E-mail: MANDAI.Toshihiko@nims.go.jp

Table S1. Crystallographic data of $[Mg(G4)(DPSO_2)_2][TFSA]_2$, $[Mg(EIm)_6][TFSA]_2$, $[Mg(G4)(MIm)_2][TFSA]_2$, and $[Mg(DMSO)_6][TFSA]_2$.

	$[Mg(G4)(DPSO_2)_2][TFSA]_2$	$[Mg(EIm)_6][TFSA]_2$	$[Mg(G4)(MIm)_2][TFSA]_2$	$[Mg(DMSO)_6][TFSA]_2$
Chemical formula	$C_{26}H_{50}F_{12}MgN_2O_{17}S_6$	$C_{34}H_{48}F_{12}MgN_{14}O_8S_4$	$C_{44}H_{68}F_{24}Mg_2N_{12}O_{26}S_8$	$C_{16}H_{36}F_{12}MgN_2O_{14}S_{10}$
Formula weight	1107.35	1161.37	1942.20	1053.38
Crystal system	Monoclinic	Monoclinic	Triclinic	Triclinic
Space group	$P2_1/n$	$P2_1/c$	P	P
a / Å	16.5803(8)	11.0919(5)	14.2221(4)	8.3553(3)
b / Å	16.0637(7)	11.1816(6)	16.1560(4)	11.6440(4)
c / Å	18.4302(8)	20.2849(11)	20.0391(6)	12.2554(4)
α / º	90	90	96.153(2)	111.290(3)
β / º	107.544(5)	98.442(5)	109.150(2)	98.550(3)
γ / º	90	90	109.657(2)	100.341(3)
V / Å^3	4680.4(4)	2488.6(2)	3971.8(2)	1062.74(7)
Z	4	2	2	1
D_{calc} / g cm^{-3}	1.571	1.550	1.624	1.646
μ / mm^{-1}	0.419	0.3106	0.375	0.640
Temp. / ºC	−150	−150	−150	−150
Reflections collected	64072	31278	81029	15050
Independent reflection, R_{int}	12438, 0.1001	6609, 0.0661	19017, 0.0954	4901, 0.0613
R_1 [$I > 2\sigma(I)$]	0.0762	0.0468	0.0615	0.0440
wR_2 (all data)	0.1972	0.1251	0.1842	0.1213
GooF	1.057	1.021	1.067	1.097
CCDC	1909206	1900782	1900781	1900780

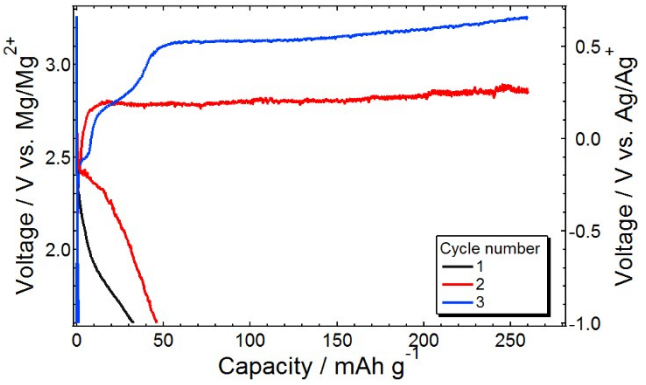

Figure S1. Capacity-unlimited galvanostatic charge–discharge curves of [Mg | hybrid electrolyte | $MgCo_2O_4$] cell measured at 100 ºC.

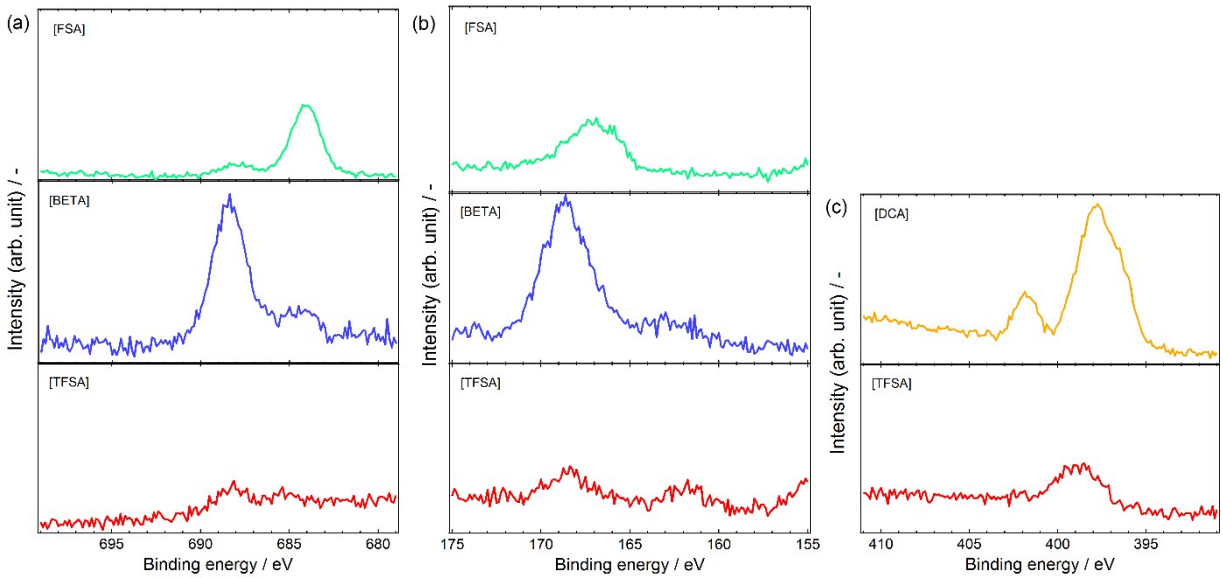

Figure S2. Narrow scan XPS spectra of the surface of magnesium strips soaked in a series of ILs with different amide-type anions for 24 h at 100 °C. (a) F1s, (b) S2p, and (c) N1s spectra.

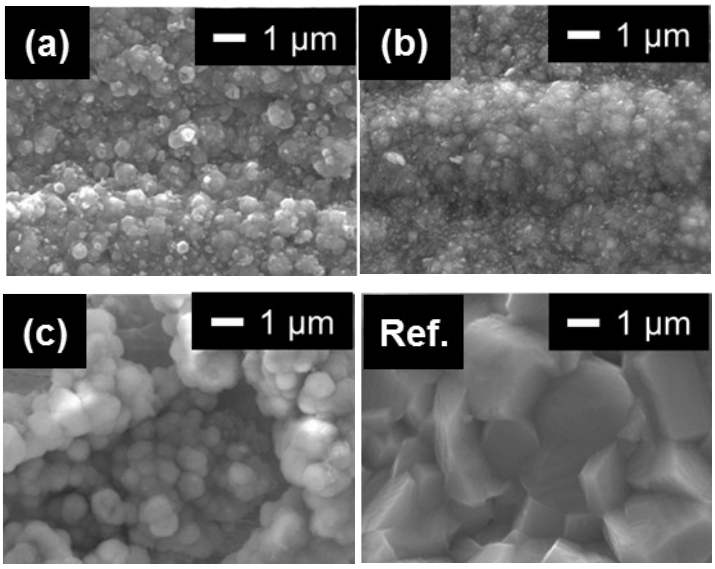

Figure S3. SEM images of deposits obtained from the mixture of Grignard reagent C_2H_5MgCl/THF with (a) $[PYR_{13}][TFSA]$, (b) $[PYR_{13}][BETA]$, and (c) $[PYR_{13}][FSA]$ by potentiostatic polarization at −0.7 V *vs*. Mg^{2+}/Mg for 1 h at ambient temperature. The image of the deposits from (d) C_2H_5MgCl/THF was also included as a reference. The subsequent EDX analysis on the specific spots indicates the magnesium concentration to be 88.6, 44.1, 29.5, and 92.1% for the electrolytes with $[TFSA]^-$, $[BETA]^-$, $[FSA]^-$, and that without any ILs, respectively.

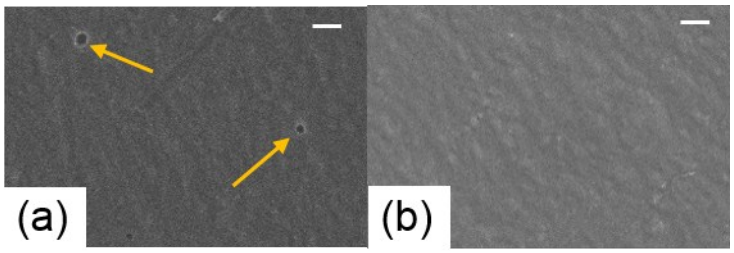

Figure S4. SEM images of Al current collectors after polarization at 3.0 V for 1 h in (a) 0.5 mol dm^{-3} hybrid $Mg[TFSA]_2$/G4-$[PYR_{13}][TFSA]$ and (b) 0.5 mol dm^{-3} $[Mg(G4)][TFSA]_2/[PYR_{13}][TFSA]$. The scale bars in each figure indicate 10 μm. Arrows in the SEM images point to pits generated by anodic dissolution.

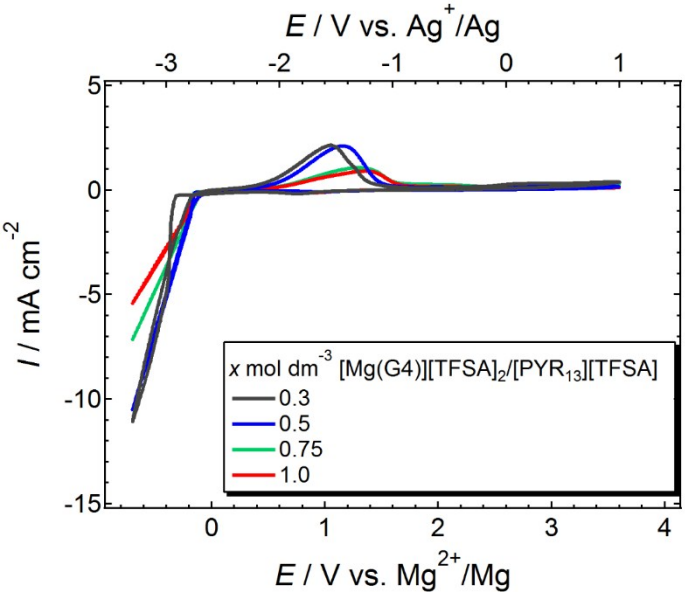

Figure S5. Concentration dependence of electrochemical activity for $[Mg(G4)][TFSA]_2/[PYR_{13}][TFSA]$ on Pt electrode at a scan rate of 50 mV s^{-1} at 100 °C.

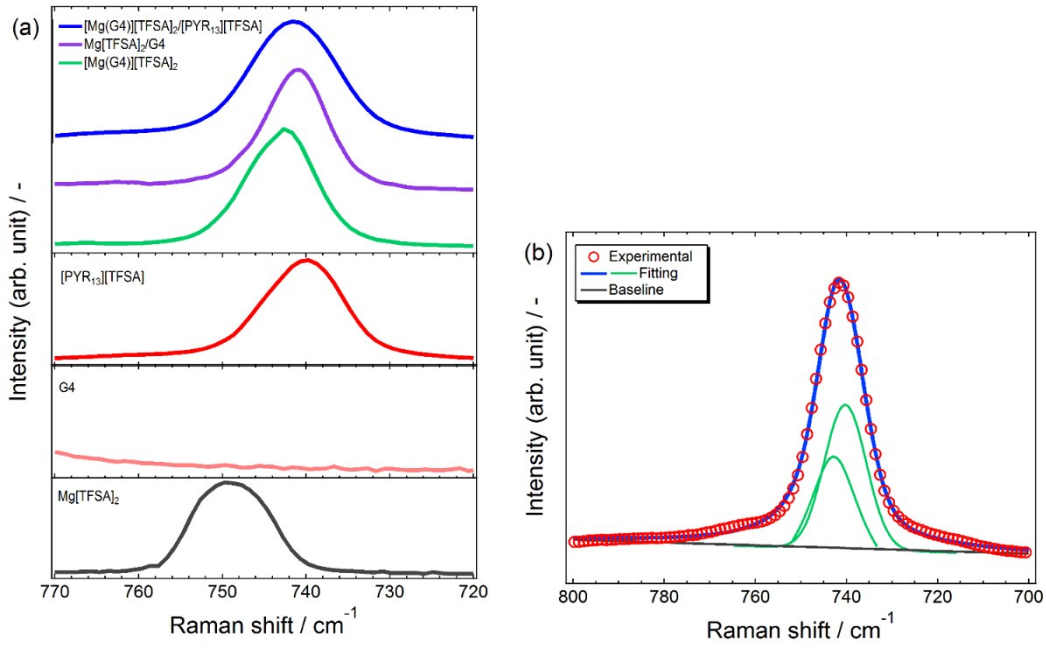

Figure S6. (a) Raman spectra of the studied electrolytes and the ingredients recorded at ambient temperature. The spectral range was adopted for the coordination state of $[TFSA]^-$ (720–770 cm^{-1}). (b) Result of spectral deconvolution for $[Mg(G4)][TFSA]_2/[PYR_{13}][TFSA]$ by using Voigt function. The spectrum was deconvoluted into two components located at 739 and 744 cm^{-1}.

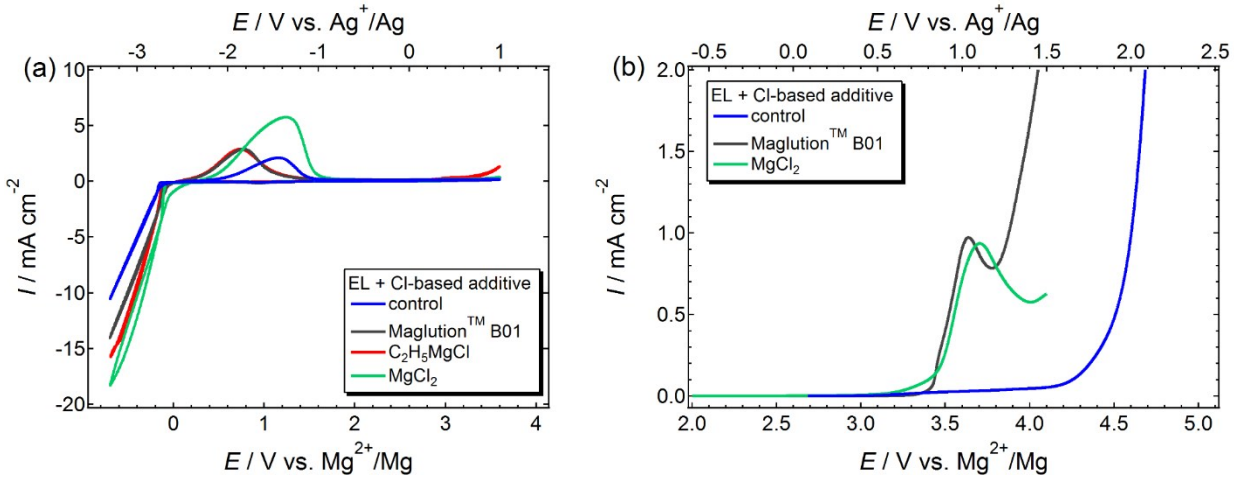

Figure S7. (a) CVs and (b) LSVs of 0.5 mol dm^{-3} [Mg(G4)][TFSA]$_2$/[PYR$_{13}$][TFSA] with Cl-based additives.

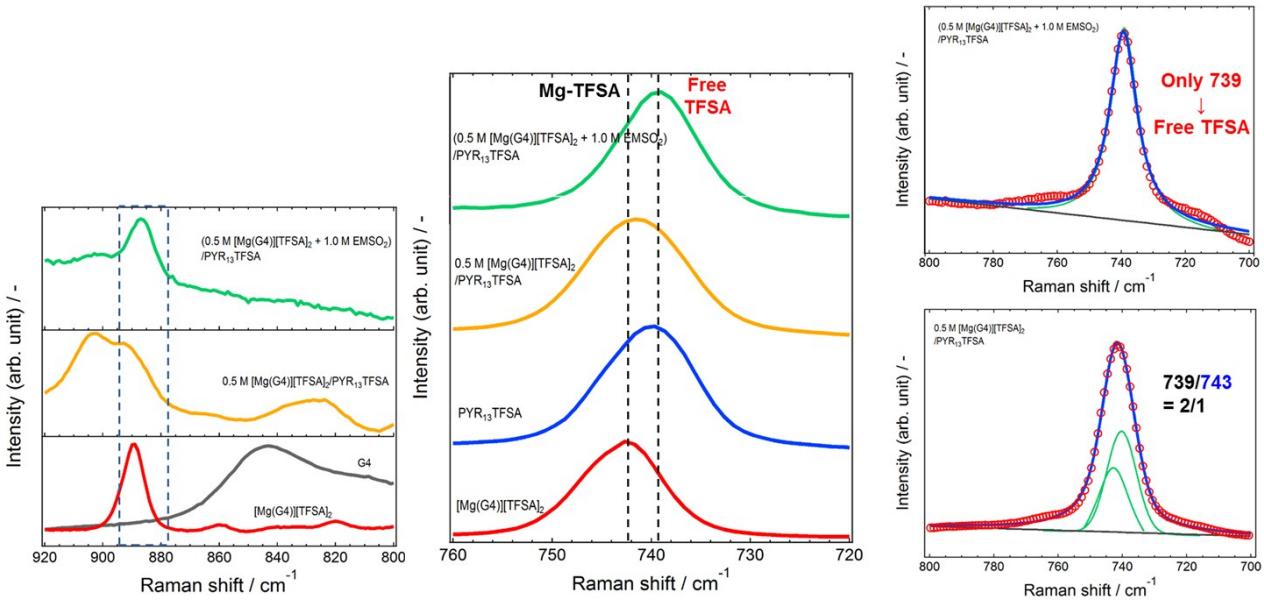

Figure S8. Raman spectra of the IL-based electrolytes incorporating the modified Mg[TFSA]$_2$ complex as a supporting salt recorded at ambient temperature. The spectral range was adopted for the coordination state of G4 (left: 920–800 cm^{-1}) and [TFSA]$^-$ (center: 720–770 cm^{-1}). Result of spectral deconvolution for (upper right) [Mg(G4)(EMSO$_2$)$_2$][TFSA]$_2$/[PYR$_{13}$][TFSA] and (lower right) [Mg(G4)][TFSA]$_2$/[PYR$_{13}$][TFSA] by using Voigt function.

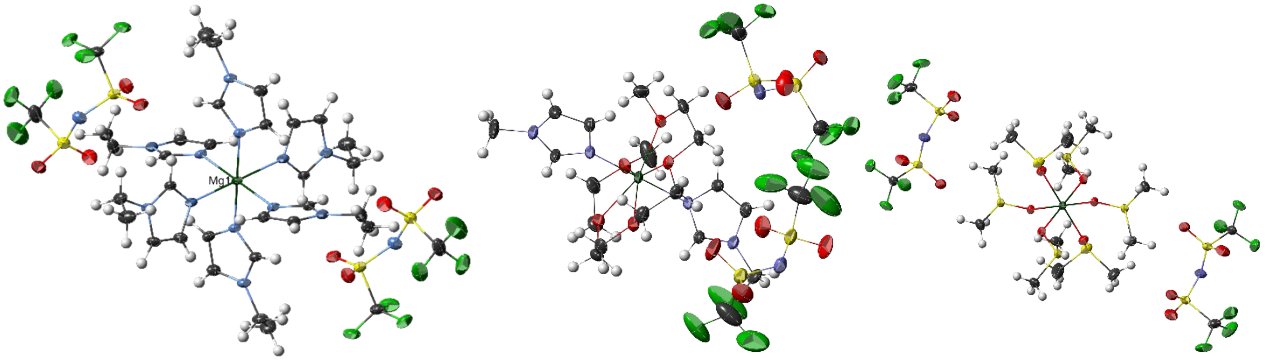

Figure S9. Thermal ellipsoid models of (left) $[Mg(EIm)_6][TFSA]_2$, (center) $[Mg(G4)(MIm)_2][TFSA]_2$, and (right) $[Mg(DMSO)_6][TFSA]_2$. The ellipsoids of non-hydrogen atoms are drawn at 50% probability level, while isotropic hydrogen atoms are represented by arbitrary spheres. Disordered atoms are not shown here. Dark green, Mg; grey, C; white, H; red, O; light green, F; light blue, N; yellow, S.

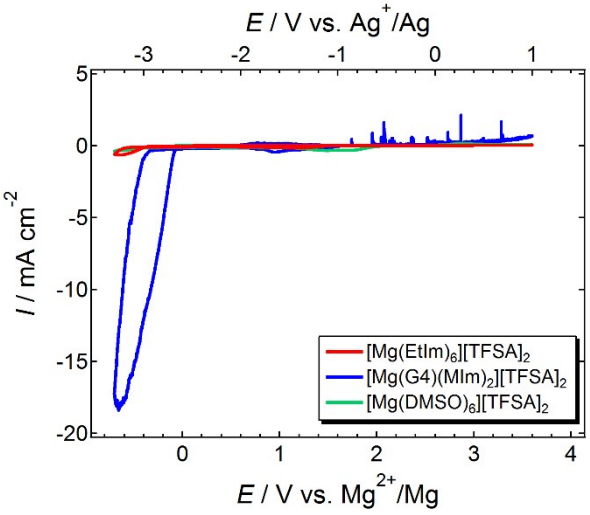

Figure S10. CVs of $[Mg(EtIm)_6][TFSA]_2$, $[Mg(G4)(MIm)_2][TFSA]_2$ and $[Mg(DMSO)_6][TFSA]_2$ complexes recorded on Pt working electrode with a scan rate of 50 mV s^{-1} at 150 °C.

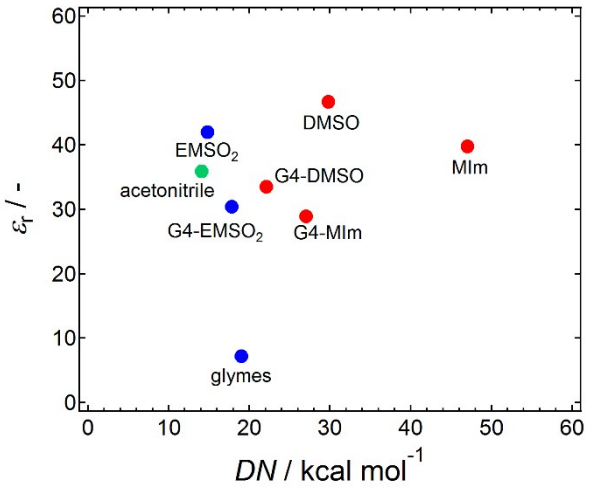

Figure S11. Mapping of *DN*s and dielectric constants (ε_r) for different ligands. The values for mixed ligand systems were derived from the simple mixture model. Ligands with *DN*s less than 20 kcal mol^{-1} (blue) would impart electrochemical magnesium plating/stripping activity for Mg[TFSA]$_2$-based electrolytes while those with *DN*s over 20 kcal mol^{-1} (red) would make complexes inactive. Acetonitrile is known to decompose at −0.2 V *vs*. Mg^{2+}/Mg but can be regarded as an effective ligand since the Mg[TFSA]$_2$/acetonitrile electrolyte supports reversible magnesiation/de-magnesiation of Bi/Mg_3Bi_2 (green) (ref. No. 69 of the main manuscript).